Journal of Bionic Engineering 14 (2017)

A Simulation of the Flight Characteristics of the Deployable Hindwings of Beetle

Jiyu Sun[1], Ruijuan Du[1], Xiaofeng Liu[2], Kamal Bechkoum[3], Jin Tong[1], Donghui Chen[1][1]

1. *Key Laboratory of Bionic Engineering* (*Ministry of Education*), *Jilin University*, *Changchun* 130022, *China*
2. *Flight Research Institute*, *Aviation University of Air Force*, *Changchun* 130025, *China*
3. *School of Computing and Technology*, *Gloucestershire University*, *Cheltenham GL*50 2*HR*, *UK*

Abstract

An insect is an excellent biological object for the bio-inspirations to design and develop a MAV. This paper presents the simulation study of the flight characteristics of the deployable hindwings of beetle, *Dorcustitanus platymelus*. A 3D geometric model of the beetle was obtained using a 3D laser scanning technique. By studying its hindwings and flight mechanism, the mathematical model of the flapping motion of its hindwings was analyzed. Then a simulation analysis was carried out to analyze and evaluate the flapping flying aerodynamic characteristics. After that, the flow of blood in the hindwing veins was studied through simulation to determine the maximum pressure on a vein surface and the minimum blood flow in flight. A number of interesting bio-inspirations were obtained. It is believed that these findings can be used for the design and development of a MAV with similar flying capabilities to a natural beetle.

Keywords: flapping, aerodynamic characteristics, deployable, hindwings, beetle, bio-inspiration

doi: 10.1016/S1672-6529(16)60392-X

1 Introduction

MAVs have been a hot research topic for last 24 years. Compared with the traditional aircrafts, MAVs have a number of advantages such as its small size, light weight, good concealment, flexibility, low cost and portability. Currently, there are three main flight modes: fixed wing, rotor, and flapping. People designed and developed different types of MAVs based on the bio-inspirations from flying creatures such as birds and insects[1]. Though there have been some progress there are limited successful applications. One of the challenges is how to reduce the size of MAVs under a low Reynolds number. It is believed that an insect is an excellent biological object for the bio-inspirations to design and develop a MAV. For example, it has been found that the wings of some insects, such as Dermaptera, Coleoptera and Blattaria, become smaller by various folding ways to protect and maintain the functionality on ground meanwhile to provide the necessary aerodynamics for flight[2–6]. It is believed that if the similar mechanism of insect wings' folding is mimicked, MAVs' wings are foldable and their performances can be considerably enhanced. A MAV with foldable wings can be either large enough to carry a required payload when fully deployed or transportable when folded and stowed[7].

It has also been found that a beetle can fly only if its hindwings are larger than its forewings (elytra). Hind- wings are membranous, and they fold under the fore- wings at non-flying states[8]. Adduction of beetles' hindwings to the body, accompanied by tucking the posterobasal wing sector or jugal lobe, is followed by semi-automatic transverse folding[9,10]. The unfolding/folding mechanism of beetles' hindwings was investigated[11–14], such as four-plate-one-spot folding mechanism[15,16] and diamond-shaped spring rotation center mechanism[17]. It is generally believed that this is achieved by the combined effect of external forces (wing base, thoracic muscle) and vein characteristics (such as vein discontinuities, venation change, and vein mem- brane elasticity)[8]. Additionally, the hemolymph runs within the veins, assisting in the wings' folding and unfolding movements[18–21]. The driving mechanism for hydraulic control of the folding and unfolding actions of beetle hind wings was proposed and investigated[19–21].

Flapping-wing flight is a type of unsteady motion. Based on numerical simulation, the characteristics of flapping kinematics of insect wing membrane were investigated[22–29]. A micro-genetic algorithm was used to numerically reconstruct the free flight motion of hawk moths[26]. Sun *et al*.[30] adopted the Computational Fluid Dynamics (CFD) method and found that the instantaneous lift peak enhancement has an important influence on the free flight or hovering of insects and that high-lift-mechanisms are effective for flapping insects to lift their own weight in flight. However, in most previous researches on flight dynamic simulations, the effect of beetle itself body feature is not

[1] Corresponding author: Donghui Chen
E-mail: dhchen@jlu.edu.cn

considered. It is believed that to fully understand the aerodynamics of in- sect flight, especially with its simple wing and body structure and high flying efficiency, it is required to not only study the principle and theory of the unsteady high-lifting mechanism but also the impact of that mechanism on the model[31]. It is believed that the further efforts should be made to study the above mentioned theory, principle and mechanism.

In previous work[19–21], the efforts were made to investigate the various hydraulic forces in the unfolding process and the hydraulic mechanism in veins of the hind wings in *Cybister japonicus* Sharp and *Dorcus titanus platymelus* (Order: Coleoptera). However, the aerodynamic properties of deployable hindwings under hydraulic control has not been fully studied, especially under semi-unsteady and unsteady flying condition. So this paper presents our research work on the above area. *D. platymelus* is selected as the biological object due to its excellent flying capability with simple wing-body structural mechanism and high efficiency.

In this paper, a 3D geometric model of the beetle is obtained using a 3D laser scanning technique. By studying its hindwings and flight mechanism, the mathematical model of the flapping motion of its hind- wings is analyzed. Then a simulation analysis is carried out to analyze and evaluate the flapping flying aerodynamic characteristics. After that, the flow of blood in the hindwings veins is studied through simulation to deter- mine the maximum pressure on a vein surface and the minimum blood flow in flight.

2 Materials and methods

2.1 3D geometric model of the beetle

To accurately simulate the flight dynamic characteristics of *D. platymelus*, it is necessary to obtain its 3D geometric model. It is important to choose a suitable scanner to digitize the beetle body and wings. The body of the sample *D. platymelus* is about 7.6 cm in length and 7 cm in width with wing in full unfolding condition. With such as dimension, considering the simulation requirement of flying dynamics of the insect, the scanner's accuracy should be in μm range. So 3D Laser scanner, Scan3Dnow, made by Taiwan Zhitai Co. was selected for digitizing the insect. The error of this scanning system is 20 μm. Since the color of the insect body and wings are black and transparent, respectively, to increase scanning accuracy and good identification effect, the insect body and wing were treated using a dye check agent. After scanning, the point cloud of the insect and its hindwings were processed using IMAGEWARE Surfacer to obtain the required geometrical data and 3D models (Fig. 1a).

It can be observed that there are bristly, scaly and hairy organs on the beetles' hindwing surfaces, but these structures are geometrically very small compared with the wing's size. So in this paper, these micro-structures can be ignored during the geometrical modelling, therefore, the surface model of the hindwing is assumed to be smooth.

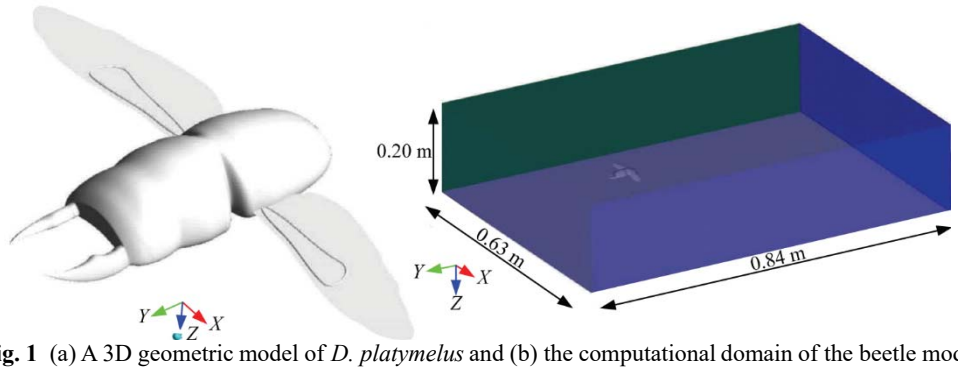

Fig. 1 (a) A 3D geometric model of *D. platymelus* and (b) the computational domain of the beetle model.

2.2 Computational domain for CFD

In a CFD analysis and simulation, a computational domain should be determined in a limited space region with the required air flow simulation environment that is not too large so that the computation task is not too heavy and the boundary interference can be considered as trivial to generate the reliable simulation results. In this paper, considering the shapes and sizes of *D. platymelus*, a cuboid is selected as the computational domain. To the best of our knowledge, there are limited published literature about how the criteria determine the relationships between the sizes of the simulation object and computational domain in bionic engineering. Fortunately, the study of vehicle external flow-field dynamics provides the valuable experience[32]. Based on this study, in our simulation, the dimension of the computational domain is 0.84 m in length (about 11 times the beetle's characteristic length), 0.63 m in width (about 9 times the beetle's characteristic width) and 0.2 m in height (about 6 times the beetle's characteristic height), as shown in Fig. 1b.

2.3 Meshing 3D models for simulation

In this paper, the Hypermesh software is used to mesh the geometrical model. Considering the overall size of the sample beetle, the beetle's surface grid is set as 0.3 mm. The density of the mesh of its head tentacles and hindwings is increased to achieve a greater precision, as shown in Fig. 2a. Three boundary layers are used on the surface of the beetle, and the total element number on the body is 10275876, with the addition of a locally refined grid (Fig. 2b).

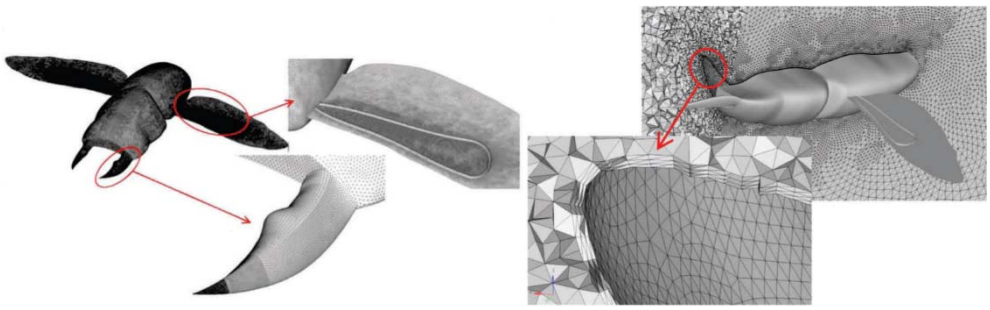

(a) (b)

Fig. 2 (a) Beetle surface computational model-3D grid; (b) locally refined grid.

2.4 Determination of boundary conditions

At the entrance of flow filed, the velocity inlet boundary conditions are established. Based on the find- ings of Wang's work on the flight characteristics of the beetle[29], flow velocity (v) is set as 0.3 m·s^{-1}, 0.6 m·s^{-1}, and 0.9 m·s^{-1}. At the outlet of flow filed, the outlet pressure boundary condition is set. Relative pressure (Rel) is set as 0 Pa and ambient atmospheric pressure (Ref) is set as 101325 Pa according to our previous experiments[19]. The beetle's surface and other wall sur- faces are set as no-slip wall (the default setting for un- steady-state flow simulation). In addition, the Shear Stress Transport (SST) k-ω turbulent model is adopted, and the low-Re corrections model is used for error correction. The SST k-ω model is used to capture the viscous flow based on the robustness of the k-ω model. The k-ω model is too sensitive to the inlet turbulence parameters. So in the mainstream area, the k-epsilon model can be used to overcome this disadvantage of the k-ω model and hence to improve the accuracy and reliability of the simulation.

2.5 Mathematical kinematics analysis of hindwings flight

The hindwing of a beetle experiences small deformation during flapping because of its flexibility (it twists into a spiral shape). But for MAVs design and development, this small deformation can be ignored[33]. So, the hindwings of the beetle are simplified as smooth rigid plates that relatively rotate about the base of the hindwings. In addition, the surrounding air is assumed to be incompressible because the flight velocityis low.

Fig. 3 shows a real insect wing's tip trajectory during flight (space trajectory curve and body trajectory curve) recorded using high-speed photography[34]. In the figure, the short line segments with directional arrows represent the wing cross sections. The solid curve is the trajectory of a wing tip modelled by regressing the middle points of all captured wing cross section line segments. It can be seen that the trajectory of the wing tip is similar to a sinusoidal curve though there are some variations in the wave crests and troughs. However, the variation is relatively small. So it is reasonable to as- sume that the trajectory of wing tip can be modelled as a sinusoidal curve in a projection plane.

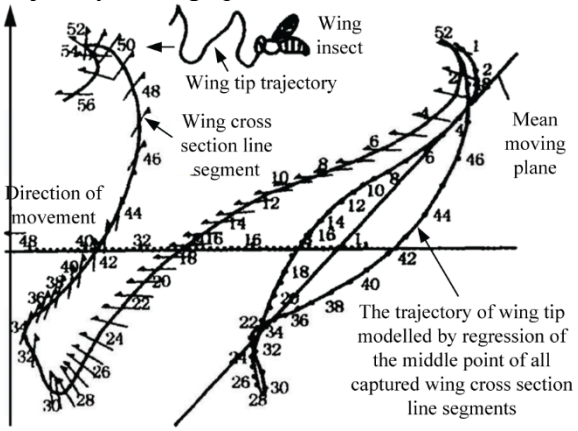

Fig. 3 The real wing tip trajectory of insect[34].

Based on the above discussion, the motion of the wing tip can be modelled as:

$$\eta = A \cdot \sin(\omega t + \theta) \tag{1}$$

Where A is the amplitude, $\omega=2\pi f$ and f is the flapping frequency, θ, is the initial phase, a constant.

The speed v of the wing tip can be obtained by differentiating Eq. (1):

$$v = A \cdot \omega \cdot \cos(\omega t + \theta) \tag{2}$$

The angular velocity ϕ of wing tip is:

$$\phi = \frac{A \cdot \omega}{L} \cdot \cos(\omega t + \theta) \tag{3}$$

where L is the distance between the wing tips and the rotation axis, as shown in Fig. 4.

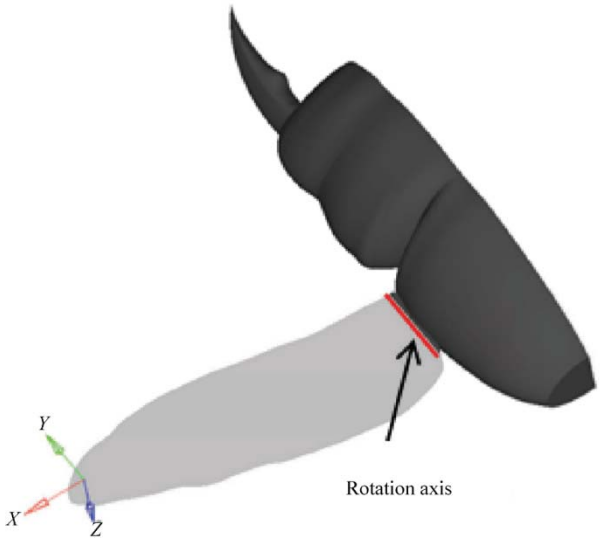

Fig. 4 The rotation axis of the *D. platymelus* hindwings.

Based on the results of the body position tracking[34], the flight parameters of the beetle are set as A=2.5 mm, L= 50 mm, θ = 0°, f=40 Hz, and $\omega=2\pi f$=251.3 rad·s^{-1}, the kinematic viscosity coefficient of the air is ν=0.15 cm^2·s^{-1}, and the density of air is ρ=1.225×10^{-3} g·cm^{-3}.

2.6 Numerical simulation of the blood circulation in a beetle's hindwing veins

The distribution of the pulses on the hindwings of the beetle is shown in Fig. 5a. It is shown that the thinner end of the pulse is a high pressure flow inlet, and the other end is a low pressure outlet. The hindwings are too thin; if the support of the vein is removed, flight is impossible. Because the veins help support the hindwings, the hindwings can flap at a certain frequency and with an amplitude and generate lift for stable flight. So it is also important to study the blood circulation in a beetle's hindwing veins.

Different grid types and qualities influence the accuracy of the simulation results. There are three factors that affect the quality of a grid: the distribution of the grid nodes, the smoothness of the mesh transitions and the shape of the grid. A reasonable density distribution of the grid nodes is based on the characteristics of physical field under consideration. The smoothness of the mesh transition is based on the different properties of the material. The change in mesh size on the boundary surface cannot be too large since the truncation errors can accumulate to unacceptable level if this change is too big. The most commonly used way for evaluating a grid is aspect ratio; the quality of the unit increases as the ratio approaches 1. The geometric model is introduced into Hypermesh and a grid mesh is generated, as shown in Fig. 5b.

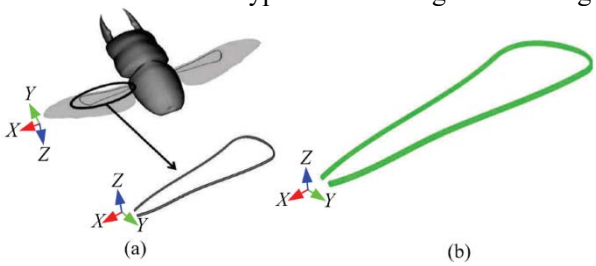

Fig. 5 (a) The pulse distribution; (b) vein grid of beetle hindwings.

The mass flow inlet boundary was used for import end, and the mass flow rate M is set to 8×10^{-10} kg·s^{-1}, 2×10^{-9} kg·s^{-1}, 4×10^{-9} kg·s^{-1}, 6×10^{-9} kg·s^{-1}, 8×10^{-9} kg·s^{-1}, 1×10^{-8} kg·s^{-1}, 2.5×10^{-8} kg·s^{-1}, 5×10^{-8} kg·s^{-1}, 7.5×10^{-8} kg·s^{-1}, and 1×10^{-7} kg·s^{-1}. The outlet pressure boundary was adopted for export, and the outlet pressure is 6 Pa. The slip wall boundary was used for the vein wall.

3 Results

3.1 Flight simulation of beetle at quasi-steady state

To obtain accurate results from the turbulence model, the generation of the boundary layer mesh is one of the most important tasks[35]. The grid in the boundary layer plays an important role in obtaining the accurate simulation results. So it is necessary to insert several boundary layers near the wall. The normal distance between the wall and the first layer grid is determined by [36]:

$$\Delta y = \frac{\nu y^+}{u_\tau} \tag{4}$$

where, ν is the kinematic viscosity coefficient, $m^2 \cdot s^{-1}$; $y^+$is the dimensionless distance from the first layer grid to the wall. u_τ is the friction velocity.

For SST model combined with the k-ε model, the allowable value of y^+ is approximately 1[36]. While the values of y^+ for the three speed conditions are all less than 1, as shown in Fig. 6. From the simulation results, it can be seen that the grid size of the body and hindwings near wall conforms to the requirements of the simulation. It is not required to further increase the density of the mesh or shrink the size.

From CFD simulation results, it can be seen that the areas of the positive pressure zone of the head and the negative pressure zone of the tail increase with the beetle flight speed, as shown in Figs. 7a–7c. A beetle's head have a positive pressure area because the head bears the direct pressure of the air flow. However, the tail of the beetle is separated from its surface at the stalling point and will cause separation of the airflow and strong disturbances. Hence, the tail of a beetle will produce a negative pressure zone. With such a pressure distribution, a beetle can fly faster due to the larger negative pressure area of the tail (Figs. 7d–7f). This is a valuable bio-inspiration when studying the flying dynamics and mechanism for the design and development of MAVs.

The maximum surface pressure of the wing is 2.6 Pa while the minimum surface pressure is −5.63 Pa in a period. That means the blood pressure of vein must be greater than the maximum pressure on the surface of the beetle hindwings, including the positive and negative pressures, so that the hindwings can flap and produce stable flight. This is another important bio-inspiration for designing the power system of wings of MAVs.

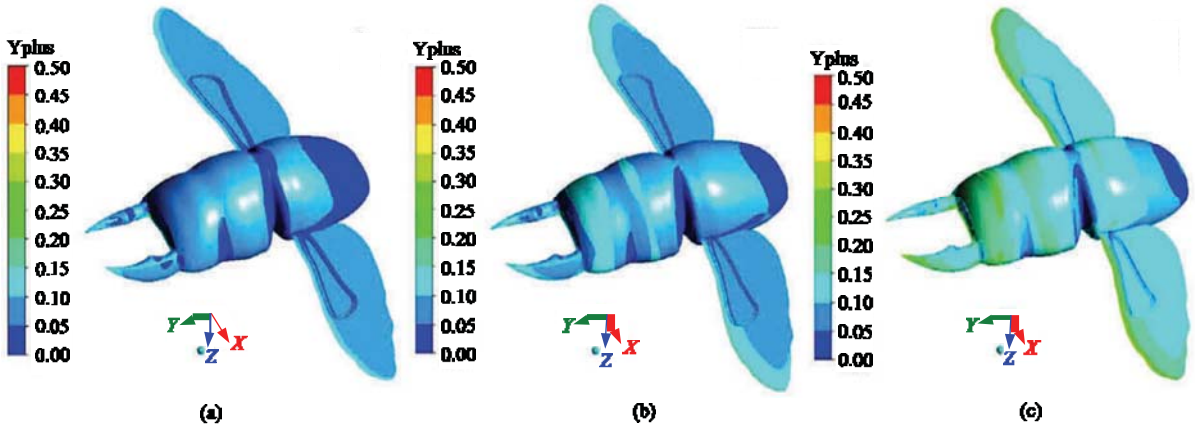

Fig. 6 The distribution of *y*+ on the surface of *D. platymelus* for the velocities of 0.3 $m \cdot s^{-1}$ (a), 0.6 $m \cdot s^{-1}$ (b) and 0.9 $m \cdot s^{-1}$ (c).

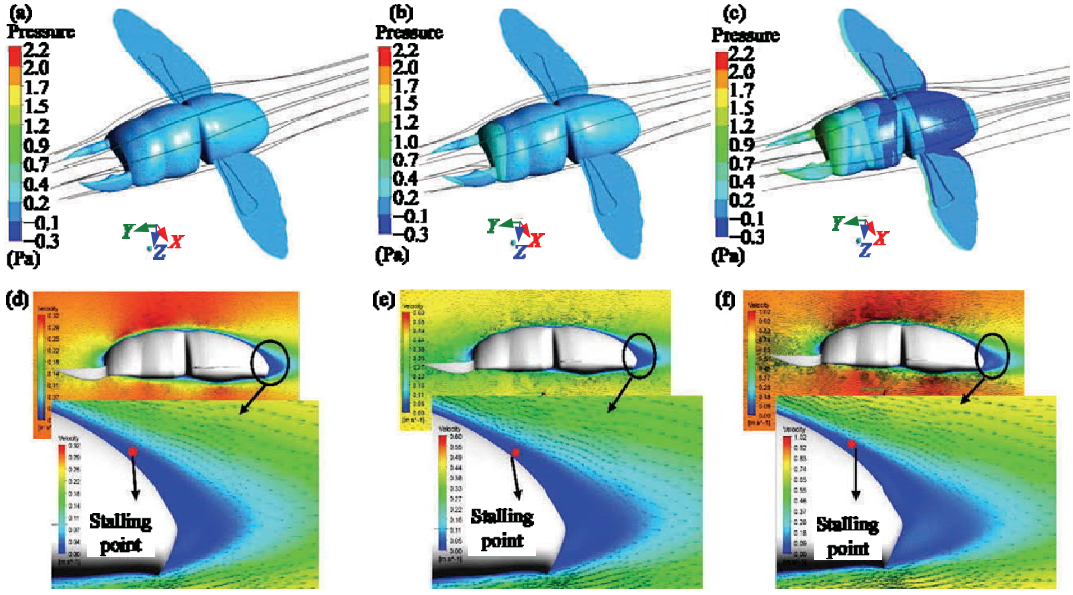

Fig. 7 Pressure distribution on the surface (a–c) and the velocity distribution of the middle section (d–f) of *D. platymelus* under the velocities of 0.3 $m \cdot s^{-1}$, 0.6 $m \cdot s^{-1}$ and 0.9 $m \cdot s^{-1}$.

Table 1 The lift of *D. platymelus* when the hindwings fully are expanded under different flying speeds

velocity ($m \cdot s^{-1}$)	0.3	0.6	0.9
Lift (N)	8.59×10^{-6}	2.32×10^{-5}	4.53×10^{-5}

Table 1 lists the lifts on the beetle when the hind- wings are fully expanded. From the simulation results, it can also be seen that the lift force of the insect under quasi-steady state is much less than its own gravity (56.15 mN), so it cannot produce enough aerodynamic lift force required for flight. Therefore, it can be concluded that insects use unsteady air currents to produce lift for flying. From Table 1, the maximum lift is 8.59×10^{-6} N. So the beetle does not meet the flight conditions. This findings conform to the findings of other studies on flying under steady flow condition at low Reynolds number range [27,37]. Wootton [12] suggested that the flying capabilities and various flight skills of insects are mostly due to that there are various wing types and complex wing movement patterns. Their wings with high flapping frequency and diverse motion patterns in flight will produce the local unsteady airflow that is different from ambient air. So it is important to fully understand the effect of the unsteady-state aero dynamics on beetle flying performances, its flying mechanism and characteristics. Therefore, section **3.2** presents the simulation of deployable hindwing of *D. platymelus* with hydraulic veins in unsteady state.

3.2 Flight simulation of beetle at unsteady state

According to Eq. (1), the motion of the wing tip can be considered as a sine function, during a cycle (T). When t=0, the surface pressure changes over the body and wing surfaces of the beetle. The pressure under the surface of the hindwing is the largest (Fig. 8a). When $t=T/4$, the maximum pressure position on the lower surface of the hindwing gradually move towards the direction of the hindwing tip (Fig. 8b). At $t=T/2$, there is a negative pressure under the surface of the hindwing (Fig. 8c). At $t=3T/4$, the range of the negative pressure of the lower surface of the hindwing further in- creased and the value of this negative pressure is −5.27 Pa (Fig. 8d).

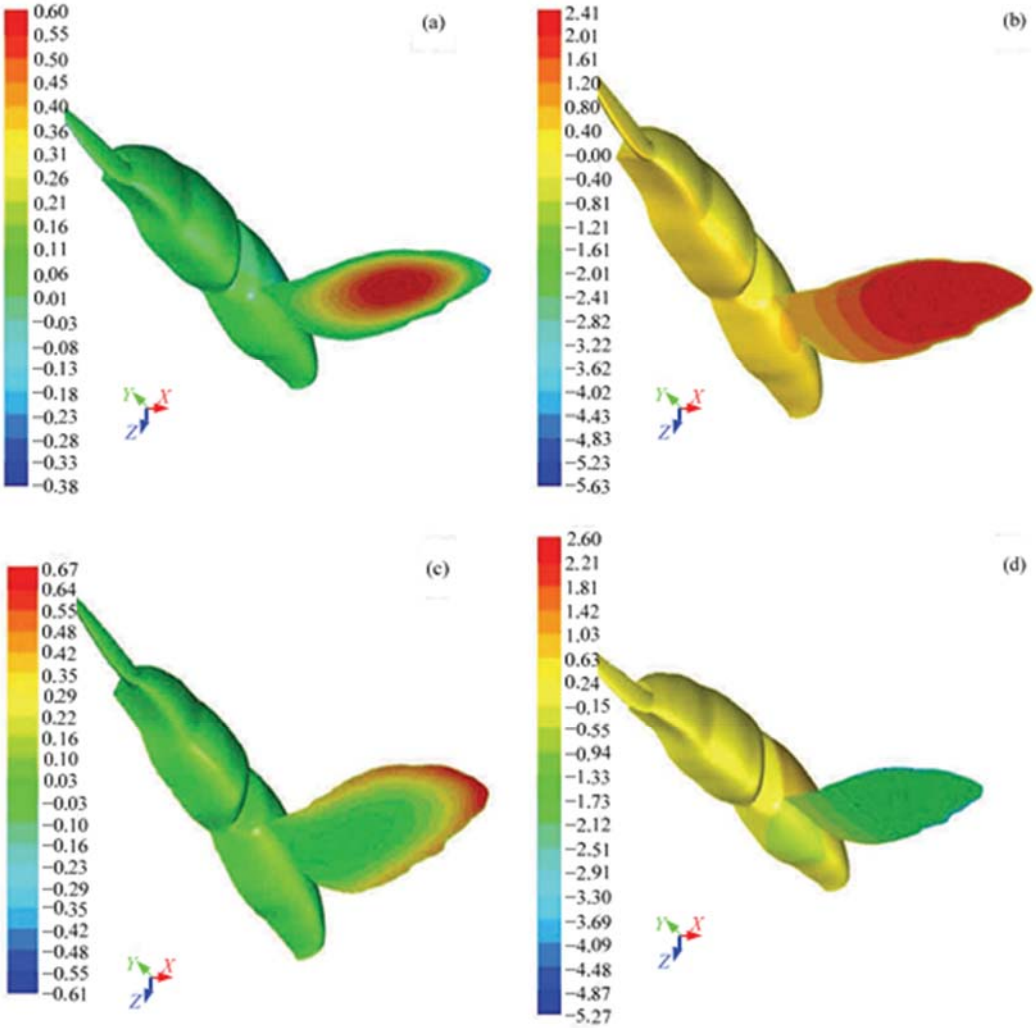

Fig. 8 The surface pressure distribution of *D. platymelus* hindwings during a flight cycle (t=0, $T/4$, $T/2$ and $3T/4$).

For flat or twisted finite rotor blades or low aspect ratio wings however, the lift coefficient ($C_L(r)$, r is the velocity of the wing at any span-wise location) may be substantially affected by a local variations in sectional inflow leading to a span-wise variation in effective angles of attack from base to tip. This effect has to be determined by

empirical measurements[38]. In this paper, the hindwings is considered as a rigid body, so the lift coefficient (C_L)[39] of *D. platymelus* is

$$C_L = \frac{F_L}{\frac{1}{2}\rho U^2 S} \tag{5}$$

The drag coefficient (C_D)[39] of *D. platymelus* is

$$C_D = \frac{F_D}{\frac{1}{2}\rho U^2 S} \tag{6}$$

where, F_L is lift force, F_D is drag force, S is the projected area along the flight direction, and U is flapping velocity. When the beetle is in flight, its speed is variable.

Fig. 9 shows C_L and C_D in the flapping cycle of insects over time. When the computation time is more than 13 cycles, the periodic change of lift and drag forces become stable. When the beetle first begins to fly, C_L changes dramatically. The C_L curve is similar to the sine curve though the peak decreases slowly and gradually becomes stable. In one cycle, wings have two C_D peaks: one is in the first half cycle of flapping, namely in the process of its flapping up; the other is in the second half cycle, namely the process of flapping wing flutter. The second peak is significantly greater than the first peak. It is necessary to point out that in the up and down of flapping, the two peaks alternately presents. Since the flapping cycle is very short, beetles get more stable lift force in flight. This is the important bio-inspiration learnt from beetle flying. That means that the flying mechanism of MAVs should be able to produce an alternative lift force in a short flapping cycle.

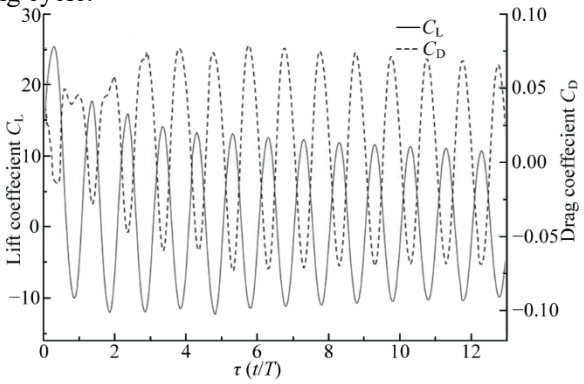

Fig. 9 The change of C_L and C_D with time for the *D. platymelus* hindwings.

In order to analyze whether the lift force obtained by numerical simulation is bigger than the gravity of the beetle in suspension, the force acting on the beetle in one cycle is analyzed. By simulation, the average C_L of one cycle is 1.08, $U=0.58L\phi_n$=10.84 m·s^{-1}[40]. One beetle hindwing area is 26.15 cm^2. When beetle completely extends its hindwings during flight, this value can be used as its projected area. The lift force produced by each wing bears half of the weight of the beetle. So S=52.3 cm^2, F_L can be calculated by Eq. (5), $F_L = \frac{1}{2}\rho U^2 S C_L$ = 376.42 mN. The weight of the beetle is about 5.73 g. So, F_L will be about 6.70 times the weight of the beetle. Therefore, the lift force is more than the weight of the beetle in suspension flying.

From the above analysis, if a MAV is designed from the findings of this simulation study, it is possible that this kind of MAV may have a considerable payload capability, as discussed in Ref. [7].

3.3 Simulation of the blood circulation in the vein of beetle's hindwings

Sections **3.1** and **3.2** present the simulation resultsof the flying aerodynamics of *D. platymelus*, especially its hindwings and find that there is a relationship be- tween the lift force and blood circulation in the vein of beetle's hindwings. So, this section presents the analysis of the relationship between blood flow and vascular surface pressure. In Fig. 10, when the blood mass flow at the entrance (M_e) is 8×10^{-10} kg·s^{-1}, the maximum pressure on the surface of the vein (P_{vmax}) is only 6.0585 Pa. As M_e decreases, P_{vmax} decreases and the pressure at the inlet side decreases as well. When M_e is zero, P_{vmax} is only 5.998 Pa, lower than the outlet pressure. Under that pressure, the blood will flow in the opposite direction which is impossible situation. So the minimum of M_e could not be zero. In contrast, as M_e increases, P_{vmax} increases linearly. The relationship between P_{vmax} and M_e can be regressed as linear. The linear regression function is

$$P_{v\max} = 0.0736M_e + 5.998 \tag{10}$$

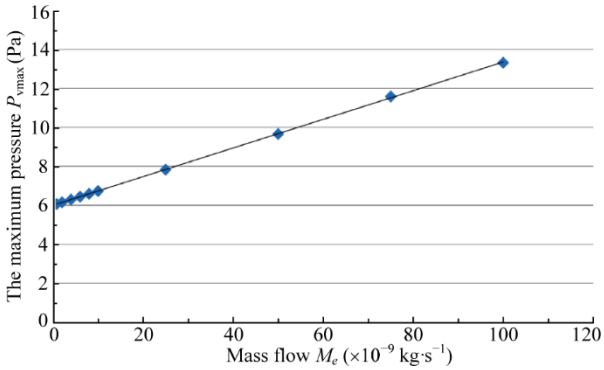

Fig. 10 The maximum pressure on the surface of the vein (P_{vmax}) changing with the blood mass flow at the entrance (M_e).

For $M_e = 1\times10^{-7}$ kg·s^{-1}, the pressure distribution on the surface of the vein is shown in Fig. 11. As shown in Fig. 11, the entry side pressure is the largest (13.3147 Pa). As the blood flows in the vein, the surface pressure of the vein decreases, and when the blood reaches the outlet, the pressure on the surface of the vein is the same as that of the outlet (6 Pa).

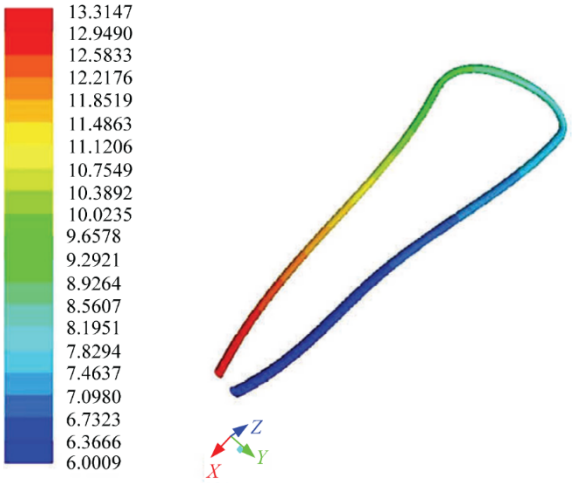

Fig. 11 The distribution of the surface pressure on the vein.

4 Discussion

A lot of efforts have been made to employ the scientific and rigorous research methods and technologies for investigating the flight mechanism of insect in recent years. For example, the trajectory of wing tip was captured[41] and the unsteady flow of wings caused by wing's flutter was investigated[42]. These findings can be used to explain the special phenomena of the high lift force generation of a flying beetle. But the current re- search is still in its infancy. To the best of our knowledge, there is not a complete set of systematic theory to explain the mechanism of insect flight including unsteady aerodynamics of insects' flight, flying control mechanism, characteristics of wings' motions and changes of airfoil, *etc*. The key point of the fully understanding of flapping flying principle is the knowledge of how a beetle uses the above features to achieve the flapping flight. This kind of knowledge can help us to design and develop a MAV that can fly like a beetle.

Our current understanding of flight control of in- sects with deployable wings is very limited. The perceptual knowledge from the data acquired from experiments is the necessary foundation for understanding the beetle flapping flight. But it is impossible to fully understand why a beetle can fly efficiently and has a big payload capability only through time-consuming and expensive experiments. Under beetle's specific flying condition, the specific lift force on the wing is needed. To provide the lift force, the blood needs to flow at specific rate, which contributes to specific pressure on the vein surface.

In order to establish the reasonable theory and principle of beetle flapping flying, it is important and necessary to carry out theoretical analysis and numerical simulations. However, this is a challenge and very difficult task. Despite the existing 3D models and simulation models of the beetle flying cannot represent all insects with deployable wings in nature, it is worthy to obtaining some findings about the mechanism and characteristics of flapping flight of beetles. This effort will eventually lead to the design and development of a MAV with similar flying capabilities with a natural beetle.

From our simulation study of semi-steady and un- steady flapping flight of *D. platymelus*, the following bio-inspirations can be learnt:

(1) A beetle's head has a positive pressure area. However, the tail of a beetle produces a negative pressure zone.

With such a pressure distribution, a beetle can fly faster due to the larger negative pressure area of the tail (Figs. 7d–7f). This is a valuable bio-inspiration when studying the flying dynamics and mechanism for the design and development of MAVs.

(2) The blood pressure of vein of the beetle must be greater than the maximum pressure on the surface of the beetle hindwings, including the positive and negative pressures, so that the hindwings can flap and produce stable flight. This is an important bio-inspiration for designing the power system of wings of MAVs.

(3) From our simulation results, it was found that two peaks of C_D alternately appear in flapping down and up process. Since the flapping cycle is very short, beetles get more stable lift force in flight. This is an important bio-inspiration learnt from beetle flying. It means that the flying mechanism of MAVs should be able to pro- duce an alternative C_D in a short flapping cycle.

(4) Under the unsteady flying state, the generated lift force is more than the weight of the beetle in suspension flying. So, if a MAV is designed based on the bio-inspirations from this simulation study, it is possible that this kind of MAV can have a considerable payload capability. This consists with that found in Ref. [6].

5 Conclusion

This paper presents the simulation study of the flight characteristics of the deployable hindwings of beetle, *D. platymelus*. A 3D geometric model of *D. platymelus* was obtained using a 3D laser scanning technique. By studying its hindwings and flight mechanism, the mathematical model of the flapping motion of its hindwings was analyzed. Then a simulation analysis was carried out to analyze and evaluate the aerodynamic characteristics of flapping flight. After that, the blood flow in the hindwing veins was studied through simulation to determine the maximum pressure on a vein surface and the minimum blood flow in flight. A number of interesting bio-inspirations were obtained, as discussed in section **4**. It is believed that these findings can be used to design and develop a MAV with similar flying capabilities with a natural beetle.

It was observed that the structure of a beetle's hindwing is flexible. That means that there should be some micro to smaller-level structural movement during flying. This kind of movement may play a considerably important role in beetle flying, such as changes of the aerodynamic characteristics in wing-air system, which could lead to the higher lift force on wings, reduced air resistance. This might be the area for the future research. It is believed that some meaningful bio-inspired findings can be obtained for future MAV design and development.

Acknowledgment

This work is supported by National Natural Science Foundation of China (No. 31672348), China-EU H2020 FabSurfWAR project (No. S2016G4501 and 644971), and 111 project (B16020) of China.

References

[1] Valavanis K P, Vachtsevanos G J. MAVs and bio-inspired UAVs: Introduction. *Handbook of Unmanned Aerial Vehi- cles*, 2015, 1301–1303.

[2] Luo Y H, Zhang D Y, Liu Y F. Recent drag reduction de- velopments derived from different biological functional surfaces: A review. *Journal of Mechanics in Medicine and Biology*, 2015, **16**, 1630001.

[3] Forbes W. The wing folding patterns of the Coleoptera(continued). *Journal of the New York Entomological Society*,1926, **34**, 91–139.

[4] Hammond P M. *Wing-Folding Mechanisms of Beetles*, *with Special Reference to Investigations of Adephagan phylogeny* (*Coleoptera*) *Carabid Beetles*, Springer, Netherlands, 1979.

[5] Danforth B N, Michener C D. Wing folding in the Hymen- optera. *Annals of the Entomological Society of America*, 1988, **81**, 342–349.

[6] Deiters J, Kowalczyk W, Seidl T. Simultaneous optimisation of earwig hindwings for flight and folding. *Biology Open*, 2016, **5**, 638–644.

[7] Dufour L, Owen K, Mintchev S, Floreano D. A Drone with insect-inspired folding wings. *Proceedings of* 2016 *IEEE/RSJ International Conference on Intelligent Robots and Systems*, Daejeon, Korea, 2016, 1576–1581

[8] Chapman R F. *The Insects*: *Structure and Function*, Cam- bridge University Press, New York, USA, 1998.

[9] Fedorenko D N. *Evolution of the Beetle Hind Wing*, *with Special Reference to Folding* (*Insecta*, *Coleoptera*), Pensoft Publishers, Sofia, Bulgaria, 2009.

[10] Brackenbury J H. Wing folding in beetles. In Pellegrino S, Guest S D, Eds., *IUTAM-IASS Symposium on Deployable Structures*: *Theory and Applications*, Springer, Dordrecht Netherlands, 2000, 37–44.

[11] Comstock J H, Needham J G. The wings of Insects. Chapter III. The specialization of wings by reduction. *American Naturalist*, 1898, **32**, 231–257.

[12] Wootton R J, Herbert R C, Young P G, Evans K E. Ap- proaches to the structural modelling of insect wings. *Phi- losophical Transactions of the Royal Society B*: *Biological Sciences*, 2003, **358**, 1577–1587.

[13] Forbes W. How a beetle folds its wings. *Psyche*, 1923, **31**,254–258.

[14] Hammond P M. Dimorphism of wings, wing-folding and wingtoiletry devices in the ladybird, *Rhyzobiuslitura* (F.) (Coleoptera: Coccinellidae), with a discussion of inter-population variation in this and other wing-dimorphic beetle species. *Biological Journal of the Linnean Society of London*, 1985, **24**, 15–33.

[15] Haas F, Wootton R J. Two basic mechanisms in insect wing folding. *Proceedings of the Royal Society B*: *Biological Sci- ences*, 1996, **263**, 1651–1658.

[16] Muhammad A, Nguyen Q V, Park H C, Hwang D Y. Byun D, Goo N S. Improvement of artificial foldable wing models by mimicking the unfolding/folding mechanism of a beetle hind wing. *Journal of Bionic Engineering*, 2010, **7**, 134–141.

[17] Haas F, Gorb S, Blickhan R. The function of resilin in beetle wings. *Proceedings of the Royal Society B*: *Biological Sci- ences*, 2000,

267, 1375–1381.
[18] Fenci G E, Currie N. Biomimetic approach for the creation of deployable canopies based on the unfolding of a beetle wing and the blooming of a flower. In Wilson S P, Verschure P F M J, Mura A, Prescott T J (eds.), *Biomimetic and Bio- hybrid Systems*, Springer International Publishing, Barce- lona, Spain, 2015, **9222**, 101–112.
[19] Sun J Y, Ling M Z, Wu W, Bhushan B, Tong J. The hydraulic mechanism of the unfolding of hind wings in *Dorcustita-nusplatymelus* (Order: Coleoptera). *International Journal of Molecular Sciences*, 2014, **15**, 6009–6018.
[20] Sun J Y, Wu W, Ling M Z, Bhushan B, Tong J. The hydraulic mechanism in the vein of hindwing of *Cybisterjaponi- cus*Sharp (Order: Coleoptera). *Beilstein Journal of Nanotechnology*, 2016, **7**, 904–913.
[21] Sun J Y, Wu W, Ling M Z, Tong J, Ren L. Fluid analysis of vein of beetle hindwing during unfolding action. *Interna- tional Journal of Heat and Mass Transfer*, 2016, **101**, 379–386.
[22] Kesel A B. Aerodynamic characteristics of dragonfly wing sections compared with technical aerofoils. *Journal of Ex- perimental Biology*, 2000, **203**, 3125–3135.
[23] Zhao L, Huang Q, Deng X, Sane S. The effect of chord-wise flexibility on the aerodynamic force generation of flapping wings: Experimental studies. *Proceedings of* 2009 *IEEE International Conference on Robotics and Automation*, Kobe, Japan, 2009, 4207–4212.
[24] Le T Q, Truong V T, Tran H T, Park S H, Ko J H, Park H C, Byun D. How could beetle's elytra support their own weight during forward flight? *Journal of Bionic Engineering*, 2014, **11**, 529–540.
[25] Wang S, Zhang X, He G, Liu T. Lift enhancement by dy- namically changing wingspan in forward flapping flight. *Physics of Fluids*, 2014, **26**, 169–230.
[26] Hedrick T, Daniel T. Flight control in the hawkmoth *Man- ducasexta*: The inverse problem of hovering. *Journal ofExperimental Biology*, 2006, **209**, 3114–3130.
[27] Ghommem M, Calo V M. Flapping wings in line formation flight: A computational analysis. *Aeronautical Journal*, 2014, **118**, 485–501.
[28] John Y, Walker S M, Bomphrey R J, Taylor G K, Thomas A L R. Details of insect wing design and deformation enhance aerodynamic function and flight efficiency. *Science*, 2009, **325**, 1549–1552.
[29] Wang Z J. Two dimensional mechanism for insect hovering. *Physical Review Letters*, 2000, **85**, 2216–2219.
[30] Sun M, Tang J M. Unsteady aerodynamic force generation by a model fruit fly wing in flapping motion. *Journal of Experimental Biology*, 2002, **205**, 55–70.
[31] Truong Q T, Nguyen Q V, Truong V T, Park H C, Byun D Y, Goo N S. A modified blade element theory for estimation of forces generated by a beetle-mimicking flapping wing sys- tem. *Bioinspiration & Biomimetics*, 2011, **6**, 036008.
[32] Huang Y H. *Numerical Simulation of Vehicle Outflow Field and Optimization of Vehicle Body Based on CFD*, Master thesis, Hunan University, China, 2011. (in Chinese)
[33] Ellington C P. The aerodynamics of hovering insect flight. III. Kinematics. *Philosophical Transactions of the Royal Society of London. Series B*: *Biological Sciences*, 1984, **305**, 41–78.
[34] Miao W B, Cheng M L. Numerical simulation of insect flight in three-dimensional condition. *Journal of Hydrodynamics*, 2005, **20**, 859–866.
[35] *User's Manual SINDA/FLUINT General Purpose Ther mal/Fluid Network Analyzer*, version 5.3, C&R Technologies, Boulder, Colorado, USA, 2009.
[36] Smith M, Zenieh S. Trajectory control of flapping wings – Towards the development of flapping-wing technology. *Proceedings of the* 6*th Symposium on Multidisciplinary Analysis and Optimization*, Bellevue, WA, USA, 1996, 493–500.
[37] Hamdani H R, Naqvi A. A study on the mechanism of high-lift generation by an insect wing in unsteady motion at small Reynolds number. *International Journal for Numeri- cal Methods in Fluids*, 2011, **67**, 581–598.
[38] Sane S P. Induced airflow in flying insects I. A theoretical model of the induced flow. *Journal of Experimental Biology*, 2006, **209**, 43–56.
[39] Ellington C P. The aerodynamics of hovering insect flight.IV. Aeorodynamic mechanisms. *Philosophical Transactions of the Royal Society of London. Series B*: *Biological Sciences*, 1984, **305**, 79–113.
[40] Zuo D C. *Key Problems Study on Flapping-Wing Micro Aerial Vehicles*, PhD thesis, Shanghai Jiao Tong University, China, 2007. (in Chinese)
[41] Cho H K, Joo W G. The aerodynamic characteristics by the insect wing tip trajectory in hovering flight. *Transactions of the Korean Society of Mechanical Engineers B*, 2009, **33**, 506–511.
[42] Mozaffari-Jovin S, Firouz-Abadi R D, Roshanian J. Flutter of wings involving a locally distributed flexible control surface. *Journal of Sound & Vibration*, 2015, **357**, 377–408.